HOKKAIDO UNIVERSITY

| | |
|---|---|
| Title | Self-Organized Two-Dimensional Vidro-Nanodot Array on Laser-Irradiated Si Surface |
| Author(s) | Yoshida, Yutaka; Sakaguchi, Norihito; Watanabe, Seiichi et al. |
| Citation | Applied Physics Express, 4(5), 055202<br>https://doi.org/10.1143/APEX.4.055202 |
| Issue Date | 2011-05 |
| Doc URL | https://hdl.handle.net/2115/45487 |
| Rights | ©2011 The Japan Society of Applied Physics |
| Type | journal article |
| File Information | APE_4-5_55202.pdf |

Hokkaido University Collection of Scholarly and Academic Papers : HUSCAP

# Title: Self-organized two-dimensional *vidro-nanodot* array on laser-irradiated Si surface


## Authors and affiliations

Yutaka Yoshida [1] Norihito Sakaguchi [2] Seiichi Watanabe [1, 2] and Takahiko Kato [3]

[1]*Division of Quantum Science and Engineering, Graduate School of Engineering, Hokkaido University, Kita-8, Nishi-13, Kita, Sapporo, Hokkaido 060-8628, Japan*

[2]*Center for Advanced Research of Energy and Materials & Graduate School of Engineering, Hokkaido University, Kita-8, Nishi-13, Kita, Sapporo, Hokkaido 060-8628, Japan*

[3]*Materials Research Laboratory, Hitachi, Ltd., 7-1-1 Omika, Hitachi-shi, Ibaraki-ken 319-1292, Japan*



**ABSTRACT**

**We report a periodic two-dimensional (2-D) array of uniquely shaped dotlike nanoprotrusions (NPs), which simultaneously self-organize on a Si surface under pulsed laser irradiation. The shape of the dotlike NPs can be controlled by adjusting the number of laser pulses. The flask-shaped dotlike NPs array is named a *vidro-nanodot* (VND) array. We present a detailed analysis of internal structure of VND using high-resolution electron microscopy.**

**Text**

The fabrication of dotlike NPs can be categorized into two competing methods: a bottom-up method by self-organizing or self-assembling single-molecule components into larger structures and a top-down method by breaking or patterning into smaller structures. Two-dimensional (2-D) nanostructure arrays or 3-D nano-objects such as a *wineglass* [1)] fabricated by focused-ion-beam chemical-vapor deposition (FIB-CVD) and artificial atomic objects fabricated by scanning tunneling microscopy (STM) [2-4)] are well-known examples of products fabricated using the bottom-up method for nanofabrication, i.e., an approach seeking to have smaller components (e.g., atoms or molecules) built up into more complex assemblies. Self-organized surface nanostructures induced by quantum beam irradiation, such as electron [5-7)] or ion [8, 9)] irradiation, have also been recognized to be fabricated by the bottom-up method. Although it has long been considered for the case of pulsed laser irradiation [10-16)] that the ripple structure formed as a laser-induced periodic surface structure (LIPSS) is caused by a top-down effect due to the interference between incident and scattered waves, [11, 12)] the self-organization of laser-induced surface nanostructures including dotlike nanoprotrusion (NP) array has recently been discussed in terms of a bottom-up process. In addition, an explanation that has been proposed for subwavelength LIPSS bifurcation

is the self-organization initiating from surface instabilities arising from two competing processes, namely, surface roughening due to explosions and surface smoothing due to self-diffusion. [14, 15)]

We report in this letter the discovery of a periodic array of flask-shaped NPs (hereafter, we call it a *vidro-nanodot* (VND) array) on a silicon surface, which is transiently generated by pulses-laser irradiation, as an intermediate state between primary NPs and hemispheroidal NPs (Fig. 1). The formation of such a periodic 2-D array of dotlike NPs is induced as a competitive phenomenon between top-down and bottom-up processes upon pulses-laser irradiation, [17)] causing the dotlike NP shape to change from primary NPs to hemispheroidal NPs. [18)] The change in shape is attributed to the well-studied aggregation of silicon clusters and atoms [19-24)] in a nonequilibrium state under the thermal gradient of nanosecond laser irradiation. It is then demonstrated that the shape of dotlike NPs can be controlled by adjusting the number of laser pulses (e.g., for VND fabrication, typically, 3000-4000 pulses with an energy density of 1.24 kJ/m$^2$ at low pressures).

Each specimen used in this study was an n-type Si(100) substrate (KN Platz Co., Ltd.) with a resistivity of 22-45 Ω·cm. The specimens were laser-irradiated at room temperature at a low pressure in an air environment using a Nd:YAG pulsed laser (Inlite

II Continuum Co., Ltd.) with a wavelength of 532 nm, a pulse width of 5-7 ns, and a repetition rate of 2 Hz. The laser incident conditions were fixed by placing a polarizer and a half-wave plate between the laser source and the specimen. A laser beam (diameter, 6 mm) normal to the surface was selected; the beam had an average laser energy density of 1.24 kJ/m$^2$.

After irradiation, the surface morphology of the specimens was observed by scanning electron microscopy (SEM: JEOL JSM-6500), and structural and chemical analyses were performed by transmission electron microscopy (TEM: JEOL JEM-2010F). To examine the distribution of the elemental concentration at the nanometer scale, elemental maps were acquired by scanning transmission electron microscopy (STEM: JEOL JEM-2010F EM-24015) and X-ray energy-dispersive spectroscopy (EDS: Noran Vantage). The structural observations were undertaken by TEM and EDS. Electron energy loss spectroscopy (EELS: Gatan PEELS Model-678) was also carried out using a field-emission transmission electron microscope operated at 200 kV with a parallel electron energy-loss spectrometer.

Figure 2 shows the structure of a 2-D VND array observed on a Si(100) surface after laser irradiation of 3000 pulses at a 1.24 kJ/m$^2$ average laser energy density and a low pressure (1.33 Pa). In this study, the laser incidence of the single beam is normal to the surface.

The VNDs were arrayed linearly with an interdot distance of 110-130 nm, perpendicularly to the laser polarization direction (denoted as ***E*** in the figures) with a line spacing of 530 nm, nearly the same as the laser central wavelength. The statistical results in Fig. 2(b) indicate that the VNDs are more than 30 nm with an average diameter of 50 nm.

A 2-D dotlike NPs array can be found near a local laser-irradiated region of high energy density. The area in which a VND array is observed is more than 100 $\mu m^2$. The growth of dotlike NPs differed from region to region, depending on the laser energy distribution such as the energy gradient between the central and local irradiated regions. The energy density of the local region on a surface where exceeds the threshold with a higher energy density melts during pulsed laser irradiation of 5-7 ns, followed by solidification. A dotlike NP is then cumulatively grown by changing the number of laser pulses, and the shape changes from a primary NP (<1500 pulses) and a VND (3000-4000 pulses) to a hemispheroidal NP (>5000 pulses) in 1.33 Pa with increasing number of laser shots. [17, 18)] Thus, it is suggested that the shape of dotlike NPs can be controlled by selecting the number of laser pulses.

To investigate details of the VND structure, we carried out a microscopic observation. Figure 3 shows TEM and STEM images and EDS elemental mappings of the

cross-section of a VND observed on a Si(100) substrate after irradiation with 1500 pulses at 1.24 kJ/m$^2$ in air. The VND was 50 nm in diameter and 120 nm in height on average. Its internal layer was made of Si, while its surface layer was identified to be silicon oxide from the high-angle annular dark-field scanning transmission electron microscopy (HAADF-STEM) image in Fig. 3(b) and from the EDS mapping (taken from the square part in Fig. 3(a)) in Figs. 3(c)-(e).

Figure 4 shows a cross-sectional high-resolution (HR) TEM image and the EELS profiles of a VND in Fig. 3. As shown in Figs. 4(b)-(d), the bottom part of the VND exhibits epitaxial growth; however, the upper side of the neck portion in Fig. 4(c) was non-epitaxial grown, owing to twinning crystallization. This indicates that the cooling rate of the corresponding part is markedly higher; moreover, some of the VNDs are observed to include a multiply twinned structure (MTS), e.g., an MTS with five domains as shown in Figs. 4(d) and (e), which is a well-known MTS in a Si nanoparticle. [22, 23] Figure 4(e) shows an HRTEM image of the MTS obtained by performing noise filtering using a fast Fourier transform (FFT) of the square region in Fig. 4(d). An ideal {111} twin with a fivefold MTS should mutually rotate each other by about 70.5°. Thus, the total angle of the five domains should be 352.5 degrees, resulting in a mismatch angle of 7.5 degrees. In Fig. 4(e), the angles of each rotation were about

($\theta_1$) 71.5, ($\theta_2$) 70.5, ($\theta_3$) 77.0, ($\theta_4$) 70.5 and ($\theta_5$) 70.0 degrees with common axis of [110] direction. It appears that the mismatch is relaxed by one of the domains with the introduction of elastic strain, namely, the $\theta_3$ domain in Fig. 4(e), which is in agreement with the case of the multiply twinned particle (MTP). [22, 23)]

Figure 4(f) shows the EELS profiles obtained at the points indicated by arrows *t* and *u* indicating the VND neck in Fig. 4(c). The Si L-edge spectra (t) and (u) corresponded to $SiO_2$ and bulk Si, respectively, confirming that the internal layer of the VND is silicon, and that the oxidized layer on the surface is a thin $SiO_2$ layer. The results of EDS analysis at the points indicated by arrow *s* in Fig. 4(b) and arrows *t*-*v* in Fig. 4(c) are also consistent with the HAADF-STEM and HRTEM observations.

Although its details have not been completely revealed, the mechanism of VND formation can be summarized as follows. First, Si atom clusters are produced by ablation in a local laser region and redeposited as atomic clusters fooled by irradation again with subsequent laser shots, which results in their melting and aggregation into dotlike NPs, such as primary NPs, accompanied by the formation of regular ripples. Such primary NP formation process has recently been confirmed by in situ pulsed-laser-equipped high-voltage electron microscopy (laser-HVEM). [17)] It is then considered that a primary NP array fabricated by self-organization under a radiation

field of laser light provides stable nucleation sites for further NP growth to VNDs. The radial expansive growth of VNDs indicates that the aggregation of atomic clusters predominantly occurs at the tip of primary NPs.

We demonstrated that a unique VND array is formed on a Si(100) substrate via a competitive phenomenon between top-down and bottom-up processes by pulses-laser irradiation. In this study, the line spacing and interdot distance of the ordered VND array related to laser wavelength were 530 nm and 110-130 nm, respectively. It is deduced that the ordering of VNDs perpendicularly to the ***E*** direction is attributable to the self-organization under linearly polarized laser irradiation. The dotlike NPs produced were distinguished by their primary NP and *vidro* shapes. The VNDs were 50 nm in diameter and 120 nm in height on average and covered with a thin $SiO_2$ layer, and their assembly was initiated at the tip of primary NPs. Patterned VNDs can be fabricated and dotlike NP structures can be controlled by adjusting the number of laser pulses. The freedom of selecting a 2-D nanostructure array presented in this article for the laser-assisted fabrication of 3-D nano-objects on a surface has the potential to lead to the development of novel nanodot devices.

**Acknowledgments**

The authors would like to thank Dr. Yang Zhanbing and Profs. Shigeo Yatsu, Tamaki Shibayama, Norihiko Nishiguchi and Heishichiro Takahashi for helpful discussions, and Kazuya Oosawa and Kenji Ohkubo for their experimental assistance and for operating the electron microscope.

**References**


1) J. Fujita, M. Ishida, T. Ichihashi, Y. Ochiai, T. Kaito, and S. Matsui: Nucl. Instrum. Methods Phys. Res. *B* **206** (2003) 472.

2) R. S. Becker, J. A. Golovchenko, and B. S. Swartzentruber: Nature **325** (1987) 419.

3) D. M. Eigler, and E. K. Schweizer: Nature **344** (1990) 525.

4) H. Uchida, D. H. Huang, J. Yoshinobu, and M. Aono: Surf. Sci. **287/288** (1993) 1056.

5) Y. Guan, J. D. Fowlkes, S. T. Retterer, M. L. Simpson, and P. D. Rack: Nanotechnology **19** (2008) 505302.

6) D. A. Smith, J. D. Fowlkes, and P. D. Rack: Nanotechnology **18** (2007) 265308.

7) K. Niwase, F. Phillipp, and A. Seeger: Jpn. J. Appl. Phys., Part 1 **39** (2000) 4624.

8) J. Evans, Nature **229** (1971) 403.

9) S. Facsko, T. Dekorsy, C. Koerdt, C. Trappe, H. Kurz, A. Vogt, and H. L. Hartnagel: Science **285** (1999) 1551.

10) M. Birnbaum: J. Appl. Phys. **36** (1965) 3688.

11) J. F. Young, J. S. Preston, H. M. Vandriel, and J. E. Sipe: Phys. Rev. *B* **27** (1983) 11552.

12) J. E. Sipe, J. E. Young, J. S. Preston, and H. M. Vandriel: Phys. Rev. *B* **27** (1983) 1141.

13) A. J. Pedraza, J. D. Fowlkes, and Y. F. Guan: Appl. Phys. A **77** (2003) 277.

14) O. Varlamova, F. Costache, J. Reif, and M. Bestehorn: Appl. Surf. Sci. **252** (2006) 4702.

15) F. Costache, M. Henyk, and J. Reif: J. Appl. Surf. Sci. **208** (2003) 486.

16) F. Sánchez, J. L. Morenza, R. Aguiar, J. C. Delgado, and M. Varela: Appl. Phys.

Lett. **69** (1996) 29.

17) S. Watanabe, Y. Yoshida, S. Kayashima, S. Yatsu, M. Kawai, and T. Kato: J. Appl. Phys. **108** (2010) 103510.

18) Y. Yoshida, S. Yatsu, S. Watanabe, M. Kawai, and T. Kato: Jpn. Inst. Electron Packag. **3** (2010) 57.

19) E. Blaisten-Barojas, and D. Levesque: Phys. Rev. *B* **34** (1986) 3910.

20) T. Yamasaki, T. Uda, and K. Terakura: Phys. Rev. Lett. ***76*** (1996) 2949.

21) E. Kaxiras, and K. Jackson: Phys. Rev. Lett. **71** (1993) 727.

22) S. Iijima: Jpn. J. Appl. Phys. **26** (1987) 357.

23) S. Iijima: Jpn. J. Appl. Phys. **26** (1987) 365.

24) C. L. Johnson, E. Snoeck, M. Ezcurdia, G. B. Rodríguez, S. I. Pastoriza, L. M. Liz , and M. J. Hÿtch: Nat. Mater. **7** (2008) 120.

**Figure captions**

**Fig. 1.** Schematically illustrated shape change of dotlike NP under pulses-laser irradiation. (a) Primary NP. Nanosize conical structure. (b) *Vidro-nanodot* (VND). Dotlike NP with flask shape. (c) Hemispheroidal NP of multicrystalline structure (Non epitaxially).

**Fig. 2.** Aligned dotlike NPs on Si surface after pulse laser irradiation: (a) SEM image of dotlike NP array on Si(100) surface after pulses-laser shots in low-pressure chamber (1.33 Pa) at repetition rate of 2 Hz and laser energy density of 1.24 kJ/m$^2$.
(b) Diameter distribution obtained from square portion in Fig. 2(c). SEM image (with tilted samples) of VND array with 70° tilt. (d) Magnified view of square portion in Fig 2(c). ***E*** indicates the electric field vector of the laser light on the surface under laser irradiation.

**Fig. 3.** Cross-sectional TEM and STEM images and EDS elemental mappings of aligned dotlike NPs on Si(100) surface after pulsed laser irradiation in air with 1500 pulses at repetition rate of 2 Hz and energy density of 1.24 kJ/m$^2$. A sample of the dotlike NP array is prepared along VNDs aligned perpendicularly to the ***E*** direction as

shown in Fig. 2.

(a) Cross-sectional TEM image of NPs. (b) HADDF-STEM image from square portion *b* in Fig. 3(a). (c)-(e) EDS mappings of silicon, oxygen and carbon, respectively, from VND in square portion in Fig. 3(a). The outside part was a carbon-deposited layer, as shown in Fig. 3(e), which was deposited when the cross-sectional specimens for STEM and TEM were prepared by a FIB process.

**Fig. 4.** High-resolution TEM image and EELS profile of VND structure on Si(100) surface after pulsed laser irradiation in air with 1500 pulses at energy density of 1.24 kJ/m$^2$. (b) Magnified view of square portion *b* in Fig. 4a. The inset is the HRTEM images taken from the top part, indicating the crystalline. (c) Magnified view of square portion *c* in Fig. 4(a). The inset is the HRTEM images taken from near the interface between the Si(001) substrate and the bottom part, indicating the epitaxial growth. (d) Magnified view of square portion *d* in Fig. 4(c).

(e) FFT-treated high-resolution image of obtained from square portion *e* in Fig. 4(d). A multiply twinned structure (MTS) of the neck part was clearly observed upon FFT treatment. (f) EELS profiles, (*t*) and (*u*), at surface (arrow *t*) and bottom (arrow *u*) of neck part in Fig. 4(c), respectively.

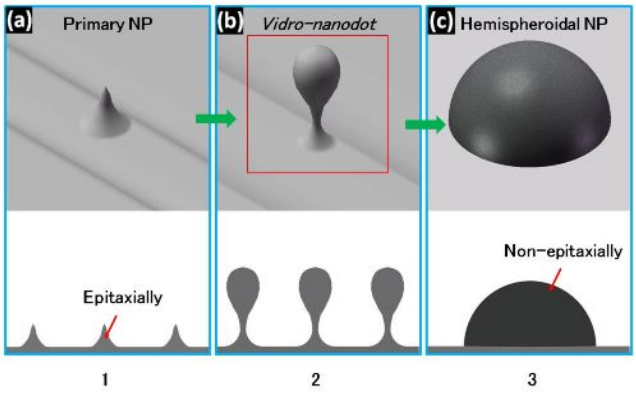


**Fig. 1. Yoshida**

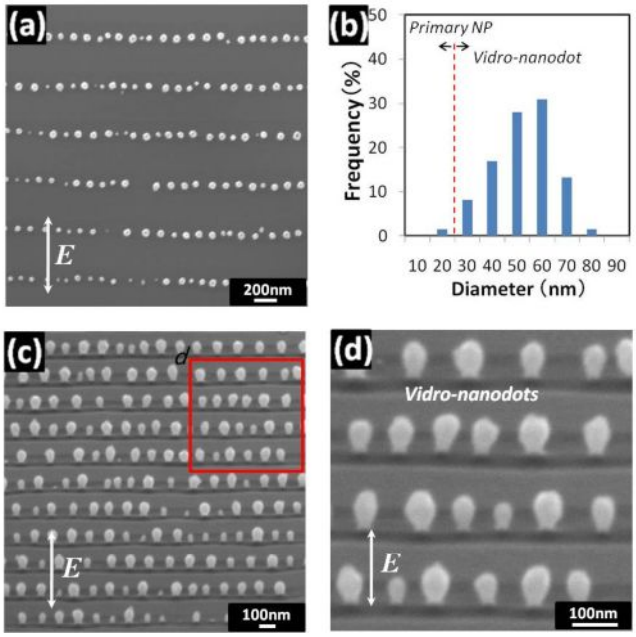


**Fig. 2. Yoshida**

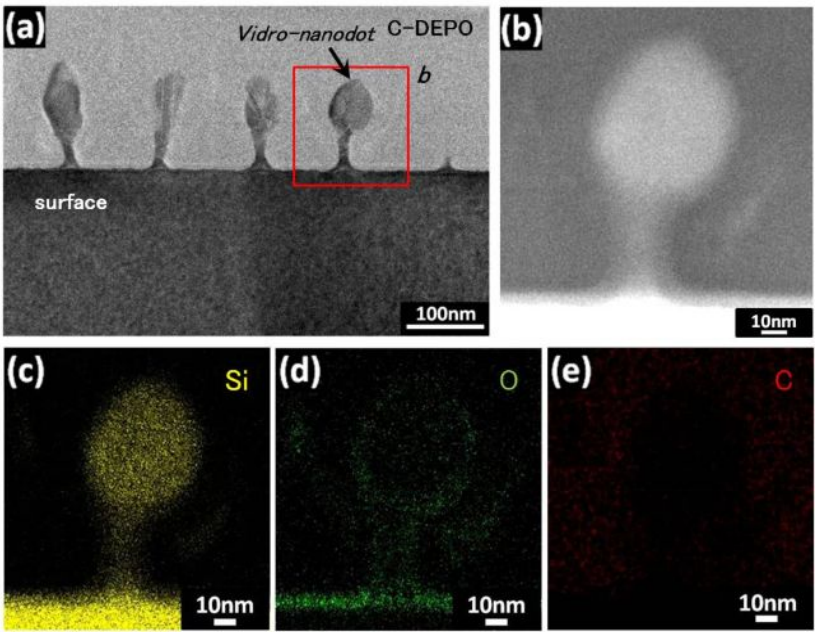


**Fig. 3. Yoshida**

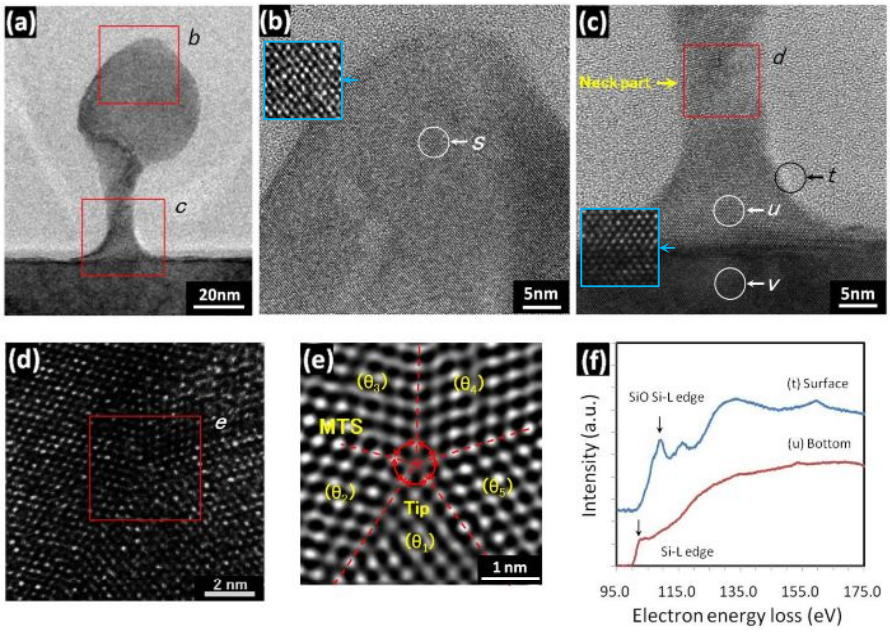


**Fig. 4. Yoshida**